

## Direct Mass Measurements of Short-Lived $A = 2Z - 1$ Nuclides $^{63}\text{Ge}$ , $^{65}\text{As}$ , $^{67}\text{Se}$ , and $^{71}\text{Kr}$ and Their Impact on Nucleosynthesis in the $rp$ Process

X. L. Tu,<sup>1,2</sup> H. S. Xu,<sup>1,\*</sup> M. Wang,<sup>1</sup> Y. H. Zhang,<sup>1</sup> Yu. A. Litvinov,<sup>3,4,1</sup> Y. Sun,<sup>5,1</sup> H. Schatz,<sup>6</sup> X. H. Zhou,<sup>1</sup> Y. J. Yuan,<sup>1</sup> J. W. Xia,<sup>1</sup> G. Audi,<sup>7</sup> K. Blaum,<sup>3</sup> C. M. Du,<sup>1,2</sup> P. Geng,<sup>1,2</sup> Z. G. Hu,<sup>1</sup> W. X. Huang,<sup>1</sup> S. L. Jin,<sup>1,2</sup> L. X. Liu,<sup>1,2</sup> Y. Liu,<sup>1</sup> X. Ma,<sup>1</sup> R. S. Mao,<sup>1</sup> B. Mei,<sup>1</sup> P. Shuai,<sup>8</sup> Z. Y. Sun,<sup>1</sup> H. Suzuki,<sup>9</sup> S. W. Tang,<sup>1,2</sup> J. S. Wang,<sup>1</sup> S. T. Wang,<sup>1,2</sup> G. Q. Xiao,<sup>1</sup> X. Xu,<sup>1,2</sup> T. Yamaguchi,<sup>10</sup> Y. Yamaguchi,<sup>11</sup> X. L. Yan,<sup>1,2</sup> J. C. Yang,<sup>1</sup> R. P. Ye,<sup>1,2</sup> Y. D. Zang,<sup>1,2</sup> H. W. Zhao,<sup>1</sup> T. C. Zhao,<sup>1</sup> X. Y. Zhang,<sup>1</sup> and W. L. Zhan<sup>1</sup>

<sup>1</sup>*Institute of Modern Physics, Chinese Academy of Sciences, Lanzhou 730000, People's Republic of China*

<sup>2</sup>*Graduate University of Chinese Academy of Sciences, Beijing, 100049, People's Republic of China*

<sup>3</sup>*Max-Planck-Institut für Kernphysik, Saupfercheckweg 1, D-69117 Heidelberg, Germany*

<sup>4</sup>*GSI Helmholtzzentrum für Schwerionenforschung, Planckstraße 1, 64291 Darmstadt, Germany*

<sup>5</sup>*Department of Physics, Shanghai Jiao Tong University, Shanghai 200240, People's Republic of China*

<sup>6</sup>*Department of Physics and Astronomy, National Superconducting Cyclotron Laboratory and the Joint Institute for Nuclear Astrophysics, Michigan State University, East Lansing, Michigan 48824, USA*

<sup>7</sup>*CSNSM-IN2P3-CNRS, Université de Paris Sud, F-91405 Orsay, France*

<sup>8</sup>*Department of Modern Physics, University of Science and Technology of China, Hefei 230026, People's Republic of China*

<sup>9</sup>*Institute of Physics, University of Tsukuba, Ibaraki 305-8571, Japan*

<sup>10</sup>*Department of Physics, Saitama University, Saitama 338-8570, Japan*

<sup>11</sup>*RIKEN Nishina Center, RIKEN, Saitama 351-0198, Japan*

(Received 8 January 2011; published 16 March 2011)

Mass excesses of short-lived  $A = 2Z - 1$  nuclei  $^{63}\text{Ge}$ ,  $^{65}\text{As}$ ,  $^{67}\text{Se}$ , and  $^{71}\text{Kr}$  have been directly measured to be  $-46\,921(37)$ ,  $-46\,937(85)$ ,  $-46\,580(67)$ , and  $-46\,320(141)$  keV, respectively. The deduced proton separation energy of  $-90(85)$  keV for  $^{65}\text{As}$  shows that this nucleus is only slightly proton unbound. X-ray burst model calculations with the new mass excess of  $^{65}\text{As}$  suggest that the majority of the reaction flow passes through  $^{64}\text{Ge}$  via proton capture, indicating that  $^{64}\text{Ge}$  is not a significant  $rp$ -process waiting point.

DOI: 10.1103/PhysRevLett.106.112501

PACS numbers: 21.10.Dr, 26.30.Ca, 29.20.db

Type I x-ray bursts occur on the surface of neutron stars accreting matter from a companion star in a stellar binary system. The accreted matter often contains hydrogen and helium, which accumulate on the neutron star surface for hours or days before igniting and burning explosively for 10 to 100 seconds causing a bright x-ray burst. The nuclear reaction sequence powering the bursts is the rapid proton capture process ( $rp$  process) [1], a sequence of proton captures and  $\beta^+$  decays near the proton drip line ending, in some extreme bursts, in the Sn region. Reliable nuclear physics input, including precise mass values, is needed for the nuclides along the  $rp$ -process path to compare models with observations of the light curve profiles and to extract quantitative information about the stellar environments [2].

It has been shown that long-lived  $rp$ -process waiting points beyond  $^{56}\text{Ni}$  can qualitatively explain the extended tails that are observed in the light curves of many x-ray bursts [3,4]. A waiting point is a nucleus near the proton drip line where a captured proton is unbound or only weakly bound and can easily be removed by photodisintegration. As a result, proton capture is effectively suppressed and the  $rp$  process has to proceed via the slow  $\beta^+$  decay. This delays the nuclear burning and leads to the extended burst tail. Three major waiting points that dominate the energy generation during the burst tail have been

identified:  $^{64}\text{Ge}$ ,  $^{68}\text{Se}$ , and  $^{72}\text{Kr}$  [5]. Their estimated long lifetimes provide the explanation for the observed burst tails. As a significant amount of hydrogen is required for the  $rp$  process to pass through the  $A = 64\text{--}72$  mass region, this has enabled astronomers to interpret long bursts as hydrogen rich, and short bursts as hydrogen poor. This is important as the amount of hydrogen affects the opacity of the atmosphere and therefore distance estimates and attempts to extract properties of the underlying neutron star from burst observations.

For a quantitative analysis of burst light curves in terms of hydrogen contents and other system parameters, the effective lifetimes of the suggested waiting points need to be known. They determine the overall processing time scale, energy generation, and the composition of the burst ashes. As all  $\beta^+$  half-lives are known, the most critical parameter becomes the proton separation energy ( $S_p$ ) of the nuclei produced by proton capture on the waiting point nucleus, which can exponentially impact the effective lifetime of the waiting point [5].  $S_p(^{69}\text{Br})$  and  $S_p(^{73}\text{Rb})$  are known to be negative based on experiments demonstrating that both  $^{69}\text{Br}$  and  $^{73}\text{Rb}$  are fast proton emitters [6,7]. This makes it likely that  $^{68}\text{Se}$  and  $^{72}\text{Kr}$  are waiting points even though  $2p$  captures can reduce their effective lifetime [5]. On the other hand, for  $^{64}\text{Ge}$ , which is the most important

potential waiting point [8] because it is encountered first, only a somewhat model dependent lower limit of  $S_p(^{65}\text{As}) > -250$  keV had been derived from the observation of the  $\beta$  decay of  $^{65}\text{As}$  [9]. A precise measurement of  $S_p(^{65}\text{As})$  is thus needed to determine to which degree  $^{64}\text{Ge}$  is a waiting point, and if it is a waiting point at all. We address this long-standing problem here by measuring accurately the mass of  $^{65}\text{As}$  ( $T_{1/2} = 128$  ms), which, together with previous measurements of the  $^{64}\text{Ge}$  mass [10], enables us to derive for the first time the experimental  $S_p(^{65}\text{As})$  value.

Recently, Penning trap mass measurements have reached some nuclides along the  $rp$ -process path [10–15]. However, the more exotic  $^{65}\text{As}$  has been out of reach so far. Attempts have been made to determine  $S_p(^{65}\text{As})$  by computing the Coulomb displacement energy (CDE) between  $^{65}\text{Ge}$  and  $^{65}\text{As}$  [16]. However, this theoretical approach needs to be verified experimentally, especially in this mass region where rapid shape changes and shape coexistence might affect nuclear masses.

The experiment has been performed at the HIRFL-CSR (Cooler-Storage Ring at the Heavy Ion Research Facility in Lanzhou) [17]. A test experiment was conducted prior to the main run described here yielding a preliminary mass excess  $\text{ME}(^{65}\text{As}) = -47\,428(\pm 530)$  keV [18]. In this Letter we report on the accurate measurement of the masses of four  $A = 2Z - 1$  nuclei  $^{63}\text{Ge}$ ,  $^{65}\text{As}$ ,  $^{67}\text{Se}$ , and  $^{71}\text{Kr}$  in a new experiment.

A primary  $^{78}\text{Kr}^{19+}$  beam of 4 MeV/u was provided by a sector focusing cyclotron. The beam passed through a carbon stripper foil placed inside the beam-transport line, and the  $^{78}\text{Kr}^{28+}$  ions were selected and injected into the main cooler-storage ring (CSRm). The  $^{78}\text{Kr}$  ions were accumulated in CSRm and then accelerated to an energy of 483.4 MeV/u. A beam intensity of up to  $\sim 10^8$  particles per spill has been achieved. The high-energy  $^{78}\text{Kr}$  beam was fast extracted from CSRm and focused upon a  $\sim 15$  mm thick beryllium production target placed at the entrance of the in-flight fragment separator (RIBLL2). The exotic nuclei were produced by projectile fragmentation of  $^{78}\text{Kr}$  and emerged from the target predominantly as bare ions. After in-flight separation of the fragments in RIBLL2, the cocktail beam of exotic nuclei was injected into the experimental storage ring (CSRe). RIBLL2 and CSRe were set to a magnetic rigidity of  $B\rho = 5.9493$  Tm to optimize the transmission of the  $A = 2Z - 1$  nuclides. Other nuclides within the acceptance of the RIBLL2-CSRe system were also transmitted and stored in CSRe. After each injection, about 20 ions were simultaneously stored in CSRe.

The revolution times  $T$  of various stored ions are related (in first order) to their mass-to-charge ratios  $m/q$  via [19]

$$\frac{\Delta T}{T} = \frac{1}{\gamma_i^2} \frac{\Delta(m/q)}{(m/q)} - \left(1 - \frac{\gamma^2}{\gamma_i^2}\right) \frac{\Delta v}{v}, \quad (1)$$

where  $\gamma$  is the relativistic Lorentz factor and  $\gamma_i$  denotes the transition point of the storage ring. In order to determine  $m/q$ , the revolution times of the ions have to be measured and the term containing their velocity spreads,  $\Delta v/v$ , needs to be minimized. For this purpose, the CSRe was tuned into an isochronous ion-optical mode [19] and the energy of the primary beam was chosen such that  $\gamma \approx \gamma_i = 1.395$  for the ions of interest. Thus, the revolution times reflect directly  $m/q$  ratios of the stored ions, independent of their  $\Delta v/v$ .

The revolution times were measured using a timing detector [20] equipped with a  $19 \mu\text{g}/\text{cm}^2$  thin carbon foil of 40 mm in diameter. Each stored ion passed through the timing detector at every revolution in CSRe. Secondary electrons released from the foil due to the passing ions were guided isochronously by perpendicularly arranged electrostatic and magnetic fields to a set of microchannel plates. The time resolution of the detector was about 50 ps, and the detection efficiency varied from 20% to 70% depending on the ion type and the number of the ions stored. The signals from the detector were sampled with a digital oscilloscope Tektronix DPO 71254 at a sampling rate of 50 GHz. The recording time was 200  $\mu\text{s}$  for each injection corresponding to  $\sim 320$  revolutions.

In this experiment, 309, 49, 104, and 28 particles were accumulated for  $^{63}\text{Ge}$ ,  $^{65}\text{As}$ ,  $^{67}\text{Se}$ , and  $^{71}\text{Kr}$ , respectively. The revolution time of each particle and its identification were determined in a way similar to that described in Ref. [19]. Figure 1 presents the histogram of the extracted revolution times for a part of the  $A = 2Z - 1$  nuclei. The nuclides whose masses were determined in this work are indicated by bold symbols.

The resolving power of CSRe mass spectrometry is mainly determined by instabilities of the magnetic fields. These instabilities cause small shifts in the revolution time

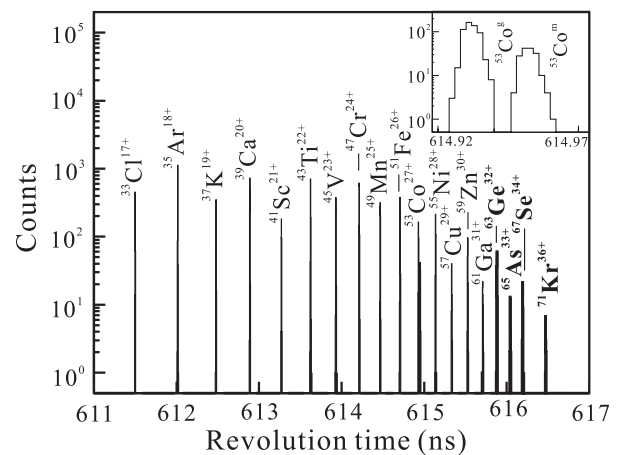


FIG. 1. The revolution time spectrum zoomed in on a subset of the  $A = 2Z - 1$  nuclides. The inset shows the well-resolved ground and isomeric [ $T_{1/2} = 247$  ms,  $E^* = 3174.3(1.0)$  keV [21]] states of  $^{53}\text{Co}$ . Our result  $E^*(^{53}\text{Co}^m) = 3202(36)$  keV is in good agreement with the literature value.

TABLE I.  $ME_{\text{CSRe}}$  and  $S_p$  values obtained in this work.  $ME_{\text{CDE}}$  values are derived from mirror nuclei ( $^{63}\text{Ga}$  [22],  $^{65}\text{Ge}$  [10],  $^{67}\text{As}$  [10], and  $^{71}\text{Br}$  [15]) using CDE [16].  $ME_{\text{AME03}}$  values are taken from AME03 [22]. Values estimated in AME03 are marked with #.

Atom	$ME_{\text{CSRe}}$ [keV]	$S_p$ [keV]	$ME_{\text{CDE}}$ [keV]	$ME_{\text{AME03}}$ [keV]
$^{63}\text{Ge}$	-46 921(37)	2210(46)	-46 945(100)	-46 910(200)#
$^{65}\text{As}$	-46 937(85)	-90(85)	-46 776(100)	-46 980(300)#
$^{67}\text{Se}$	-46 580(67)	1851(74)	-46 548(100)	-46 490(200)#
$^{71}\text{Kr}$	-46 320(141)	2184(142)	-46 025(100)	-46 920(650)

of the entire spectrum for different injections. In order to reduce the effect of these shifts, we measured the revolution time of each particle relative to the revolution time of a selected reference nuclide present in the same injection. As not all nuclides were present in each injection, we used seven reference peaks ( $^{19}\text{Ne}$ ,  $^{21}\text{Na}$ ,  $^{23}\text{Mg}$ ,  $^{25}\text{Al}$ ,  $^{27}\text{Si}$ ,  $^{29}\text{P}$ , and  $^{31}\text{S}$ ) thus creating seven independent spectra which contain 69% of all particles. The resolving power of the shift-corrected spectra is 170'000.

All the  $A = 2Z - 1$  nuclides with experimentally known masses [21,22] from  $^{33}\text{Cl}$  through  $^{61}\text{Ga}$  (except for  $^{43}\text{Ti}$  since it has a low-lying isomeric state) were used to fit  $m/q$  versus  $T$  employing a second order polynomial. The ME values of  $^{63}\text{Ge}$ ,  $^{65}\text{As}$ ,  $^{67}\text{Se}$ , and  $^{71}\text{Kr}$  were obtained and presented in Table I by extrapolating the fit function to the corresponding  $T$ . The seven subspectra and an integral spectrum have been analyzed separately and provided consistent results. In order to estimate possible systematic errors, the literature ME values have been redetermined in the analysis using a different number of reference nuclides and different extrapolation ranges. For instance, the redetermined mass values for  $^{55}\text{Ni}$ ,  $^{57}\text{Cu}$ ,  $^{59}\text{Zn}$ , and  $^{61}\text{Ga}$  (the extrapolation range is about the same as used to fit the new masses) are consistent with literature values [21,22] within  $1\sigma$ . Mainly due to the small extrapolation range (for  $^{71}\text{Kr}$  it is just  $\sim 0.76$  ns), the errors for the new masses are dominated by statistical errors. Details of the data analysis will be described in [23].

$S_p$  values for  $^{63}\text{Ge}$ ,  $^{65}\text{As}$ ,  $^{67}\text{Se}$ , and  $^{71}\text{Kr}$  were deduced using our new masses and the previously known masses of  $^{62}\text{Ga}$  [22],  $^{64}\text{Ge}$  [10],  $^{66}\text{As}$  [10], and  $^{70}\text{Br}$  [15]. We emphasize that  $S_p(^{65}\text{As}) = -90(85)$  keV. This confirms experimentally for the first time that  $^{65}\text{As}$  is unbound against proton emission at a 68.3% confidence level. Our  $S_p(^{65}\text{As})$  agrees with the limit of  $S_p > -250$  keV obtained in Ref. [9] based on the observed  $\beta$  decay and theoretical estimates of the proton penetrability.

The new experimental ME values are compared in Table I with those calculated by the CDE method [16] and those from the latest atomic mass evaluation (AME03) [22]. Good agreement between CSRe and CDE is found for  $^{63}\text{Ge}$ ,  $^{65}\text{As}$ , and  $^{67}\text{Se}$ , which confirms the predictive power of the CDE method in this mass region and shows that at least for these three nuclei the method is reliable. In the case of  $^{71}\text{Kr}$ , the CDE value differs by more

than one standard deviation from our CSRe result. The recently measured  $ME(^{71}\text{Br}) = -56\,502.4(5.4)$  keV [15], combined with  $Q_\beta(^{71}\text{Kr}) = -10\,140(320)$  keV [24], yields  $ME(^{71}\text{Kr}) = -46\,360(320)$  keV, which agrees nicely with our CSRe result of  $ME(^{71}\text{Kr}) = -46\,320(141)$  keV. The disagreement of the CDE and our values for  $^{71}\text{Kr}$  may hint at a structure change along the  $N = Z$  line at  $N = Z = 35$ . Nuclei with  $N = Z \leq 35$  are nearly spherical while the heavier ones are strongly deformed. Hasegawa *et al.* [25] have suggested that there is a sudden shape change near the ground state at  $N = Z = 35$ , which may be regarded as a (spherical to deformed) phase transition. Furthermore, Kr isotopes with  $N \approx Z$  are known to exhibit the shape-coexistent phenomenon [26,27]; for example, deformed prolate and oblate shapes compete near the ground state with comparable energies. This suggests that deformation effects and shape coexistence are the factors that future CDE calculations may need to consider.

The experimental  $S_p(^{65}\text{As})$  allowed us to determine the degree to which  $^{64}\text{Ge}$  is an  $rp$  process waiting point. Figure 2 shows regions in the temperature-density plane where proton captures reduce the effective lifetime

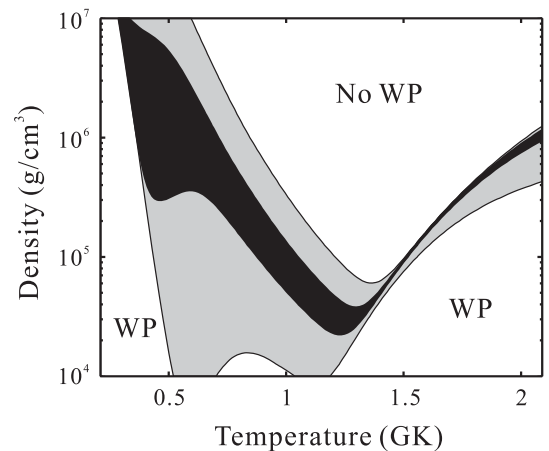


FIG. 2. Regions in the temperature and density plane where  $^{64}\text{Ge}$  is a waiting point (WP) with an effective lifetime longer than 50% of the  $\beta$ -decay lifetime. Shaded areas are deduced assuming a  $1\sigma$  variation of the AME03 mass for  $^{65}\text{As}$  (gray) and the  $^{65}\text{As}$  mass from this work (black). Results are given for a proton mass fraction of 0.7.

of  $^{64}\text{Ge}$  to less than 50% of the  $\beta$ -decay lifetime resulting in a less effective waiting point. With our new mass value the temperatures and densities needed to bypass the  $^{64}\text{Ge}$  waiting point are rather well defined. In particular, it is clear that a fairly high density in excess of  $2 \times 10^4 \text{ g/cm}^3$  will be needed. For densities below  $2 \times 10^5 \text{ g/cm}^3$  the required temperature range is rather narrow around 1.3 GK. For lower temperatures,  $^{64}\text{Ge}$  can only be bypassed at higher densities. To illustrate the importance of the mass accuracy, we also show the region obtained with a 300 keV uncertainty (AME03). Though it is bigger than the uncertainty quoted for CDE calculations of the  $^{65}\text{As}$  mass, we stress that the theoretical uncertainties were estimated from the performance of the model in other mass regions.

We have implemented our new results in a one-zone x-ray burst model [4] to explore the impact on modeled light curves. Figure 3 shows the calculated x-ray luminosity as a function of time. Varying our  $S_p(^{65}\text{As}) = -90 \text{ keV}$  within  $2\sigma$  provides essentially identical light curves demonstrating that our accuracy is sufficient to eliminate the effect of the  $^{65}\text{As}$  mass uncertainty in x-ray burst calculations. 89%–90% of the reaction flow passes through  $^{64}\text{Ge}$  via proton capture indicating that  $^{64}\text{Ge}$  is not a significant  $rp$ -process waiting point. In contrast, using the estimated upper  $2\sigma$  limit for  $^{65}\text{As}$  from AME03 ( $S_p(^{65}\text{As}) \approx -650 \text{ keV}$ ), leads to a reduction of the proton capture flow through  $^{64}\text{Ge}$  to 54% with a significant effect on the light curves (see Fig. 3).

Figure 4 shows the composition of the burst ashes. This is relevant for model calculations of the crusts of accreting neutron stars that exhibit x-ray bursts [28]. The sensitivity of the composition to the  $^{65}\text{As}$  mass uncertainty had been pointed out before [8]. A  $1\sigma$  variation of the remaining 85 keV uncertainty of  $S_p(^{65}\text{As})$  has overall a very small effect, except for a factor of 3 uncertainty in the  $A = 64$  abundance. We emphasize that the  $A = 64$  abundance is

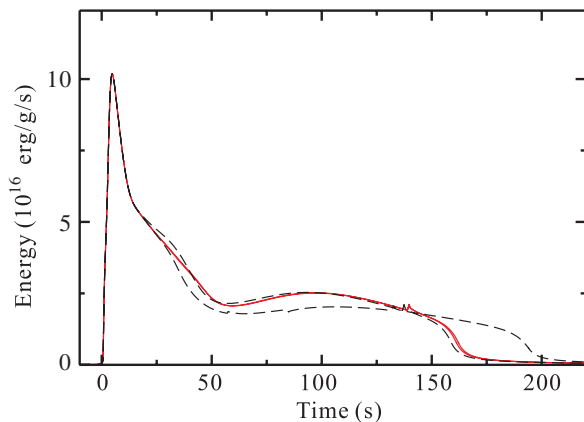


FIG. 3 (color online). Calculated x-ray luminosity in a one-zone x-ray burst model varying  $S_p(^{65}\text{As})$  within  $2\sigma$  for masses from AME03 [22] (dashed black lines) and from this work (solid red lines).

about an order of magnitude lower than the most abundant constituents of the burst ashes. If the AME03 values are used, the uncertainty of the  $A = 64$  abundance is much larger and includes the possibility of  $A = 64$  being one of the main components of the ashes. It is clear that our new data have reduced the uncertainties significantly. For the data from the AME03, the changes in the calculated abundances (see Fig. 4) are entirely due to the lower bound of  $S_p$  that causes  $^{64}\text{Ge}$  to become a significant waiting point. Interestingly this delays energy generation, resulting in high temperature conditions for a longer time and enhancement of the production of the heaviest isotopes. This is the opposite of what one might naively expect for a stronger bottleneck at the proton-unbound  $^{65}\text{As}$ .

In summary, the masses of the short-lived  $A = 2Z - 1$  nuclides  $^{63}\text{Ge}$ ,  $^{65}\text{As}$ ,  $^{67}\text{Se}$ , and  $^{71}\text{Kr}$  have been directly measured for the first time using a new implementation of the storage ring mass spectrometry. While for  $^{63}\text{Ge}$ ,  $^{65}\text{As}$ , and  $^{67}\text{Se}$  our data confirm theoretical predictions based on CDE calculations, a  $1.7\sigma$  discrepancy to theory for  $^{71}\text{Kr}$  may suggest the necessity of an experimental validation of such calculations for nuclei along the  $N = Z$  line. The measurement of the  $^{65}\text{As}$  mass provides the first experimental  $S_p(^{65}\text{As})$  value. This establishes reliably the astrophysical conditions under which  $^{64}\text{Ge}$  is an  $rp$ -process waiting point. For the particularly hydrogen-rich x-ray bursts explored in our x-ray burst model,  $^{64}\text{Ge}$  is now with certainty not a major waiting point in the  $rp$ -process in x-ray bursts. This increases the importance of possible subsequent waiting points such as  $^{68}\text{Se}$  and  $^{72}\text{Kr}$ , for which an experimental determination of  $S_p(^{69}\text{Br})$  and  $S_p(^{73}\text{Rb})$  would be desirable, though existing limits suggest these nuclei as waiting points. Our measurement has removed a major uncertainty in x-ray burst

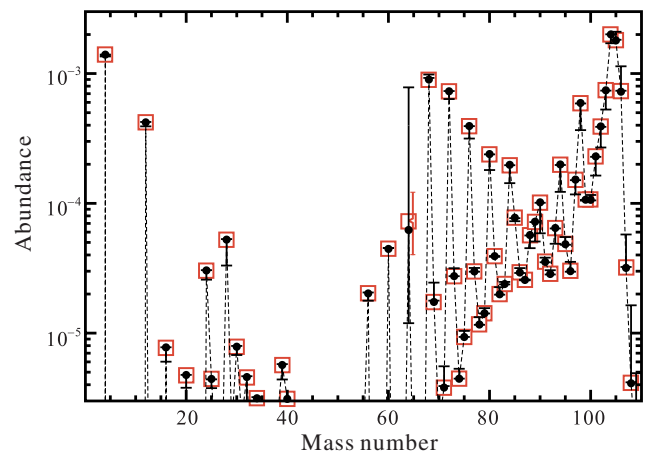


FIG. 4 (color online). The calculated abundance distribution of the x-ray burst ashes using  $S_p(^{65}\text{As})$  from AME03 (black filled circles) and from this work (red open squares). Error bars indicate uncertainties induced by the  $1\sigma$  uncertainty of  $S_p(^{65}\text{As})$ . Except for  $A = 64$ , the error bars of our new results are within the symbol size.

models and paved the way for a quantitative analysis of observed x-ray burst tails. The current results may also be of importance in the  $\nu p$  process [29,30] in neutrino driven winds in core collapse supernovae, though more work needs to be done to explore the sensitivity of this site to masses around  $^{64}\text{Ge}$ ,  $^{68}\text{Se}$ , and  $^{72}\text{Kr}$ .

This work is supported by the CAS, the NSFC (Grants No. 10925526, No. 11035007, No. 10675147, No. 10805059, No. 10875077, No. 11075103), and the Major State Basic Research Development Program of China (Contract No. G2007CB815000). H. S. is supported by NSF Grants No. PHY06-06007 and No. PHY08-22648. Y. A. L is supported by CAS (Grant No. 2009J2-23).

---

\*hushan@impcas.ac.cn

- [1] R. Wallace and S. Woosley, *Astrophys. J. Suppl. Ser.* **45**, 389 (1981).
- [2] H. Schatz and K. E. Rehm, *Nucl. Phys.* **A777**, 601 (2006).
- [3] O. Koike *et al.*, *Astron. Astrophys.* **342**, 464 (1999).
- [4] H. Schatz *et al.*, *Phys. Rev. Lett.* **86**, 3471 (2001).
- [5] H. Schatz *et al.*, *Phys. Rep.* **294**, 167 (1998).
- [6] B. Blank *et al.*, *Phys. Rev. Lett.* **74**, 4611 (1995).
- [7] A. Jokinen *et al.*, *Z. Phys. A* **355**, 227 (1996).
- [8] A. Parikh *et al.*, *Phys. Rev. C* **79**, 045802 (2009).
- [9] J. A. Winger *et al.*, *Phys. Rev. C* **48**, 3097 (1993).
- [10] P. Schury *et al.*, *Phys. Rev. C* **75**, 055801 (2007).
- [11] J. A. Clark *et al.*, *Phys. Rev. C* **75**, 032801(R) (2007).
- [12] J. A. Clark *et al.*, *Phys. Rev. Lett.* **92**, 192501 (2004).
- [13] D. Rodríguez *et al.*, *Phys. Rev. Lett.* **93**, 161104 (2004).
- [14] C. Weber *et al.*, *Phys. Rev. C* **78**, 054310 (2008).
- [15] J. Savory *et al.*, *Phys. Rev. Lett.* **102**, 132501 (2009).
- [16] B. A. Brown *et al.*, *Phys. Rev. C* **65**, 045802 (2002).
- [17] J. W. Xia *et al.*, *Nucl. Instrum. Methods Phys. Res., Sect. A* **488**, 11 (2002).
- [18] H.-S. Xu *et al.*, *Chin. Sci. Bull.* **54**, 4749 (2009).
- [19] M. Hausmann *et al.*, *Hyperfine Interact.* **132**, 289 (2001).
- [20] B. Mei *et al.*, *Nucl. Instrum. Methods Phys. Res., Sect. A* **624**, 109 (2010).
- [21] A. Kankainen *et al.*, *Phys. Rev. C* **82**, 034311 (2010).
- [22] G. Audi *et al.*, *Nucl. Phys.* **A729**, 337 (2003).
- [23] X. L. Tu *et al.* (to be published).
- [24] M. Oinonen *et al.*, *Phys. Rev. C* **56**, 745 (1997).
- [25] M. Hasegawa *et al.*, *Phys. Lett. B* **656**, 51 (2007).
- [26] E. Bouchez *et al.*, *Phys. Rev. Lett.* **90**, 082502 (2003).
- [27] Y. Sun *et al.*, *Nucl. Phys.* **A758**, 765c (2005).
- [28] S. Gupta *et al.*, *Astrophys. J.* **662**, 1188 (2007).
- [29] C. Fröhlich *et al.*, *Phys. Rev. Lett.* **96**, 142502 (2006).
- [30] J. Pruet *et al.*, *Astrophys. J.* **644**, 1028 (2006).